Accepted Manuscript

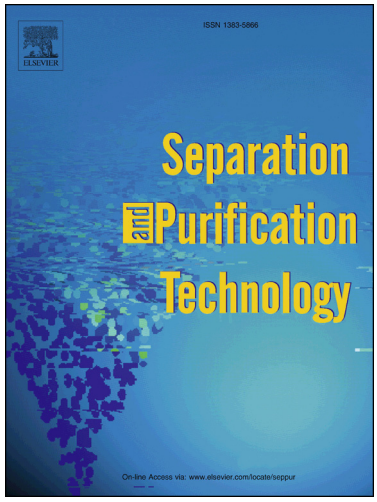

A practical approach to fixed-site-carrier facilitated transport modeling for the separation of propylene/propane mixtures through silver-containing polymeric membranes

Authors: Raúl Zarca, Alfredo Ortiz, Daniel Gorri, Inmaculada Ortiz

PII: S1383-5866(17)30047-3
DOI: http://dx.doi.org/10.1016/j.seppur.2017.02.050
Reference: SEPPUR 13582

To appear in: *Separation and Purification Technology*

Received Date: 9 January 2017
Revised Date: 24 February 2017
Accepted Date: 25 February 2017

Please cite this article as: A.R. Zarca, A. Ortiz, D. Gorri, I. Ortiz, A practical approach to fixed-site-carrier facilitated transport modeling for the separation of propylene/propane mixtures through silver-containing polymeric membranes, *Separation and Purification Technology* (2017), doi: http://dx.doi.org/10.1016/j.seppur.2017.02.050

A practical approach to fixed-site-carrier facilitated transport modeling for the separation of propylene/propane mixtures through silver-containing polymeric membranes

Authors: Raúl Zarca, Alfredo Ortiz, Daniel Gorri, Inmaculada Ortiz*.

Department of Chemical and Biomolecular Engineering. University of Cantabria, Av. Los Castros 46, 39005 Santander, Spain

*corresponding author: ortizi@unican.es

Submitted to *Separation & Purification Technology*

February 2017

Revised manuscript

Abstract

In this work, a new consistent mathematical model for the description of the olefin flux through Ag^{+}-containing polymeric dense membranes is proposed. A fixed site carrier "hopping" parameter acting as an effective permeability for this specific transport phenomenon is defined and calculated for the first time. This study reports a simple and versatile approach that can be incorporated into future models to simulate the more complex mobile/fixed hybrid mechanism acting in composite membranes.

Furthermore, in order to validate the model, the proof of concept has been carried out with PVDF-HFP/$AgBF_4$ facilitated transport membranes. The experimental analysis has been performed by the continuous flow permeation method through flat membranes containing increasing silver loads, from 17 to 38 % w/w at olefin partial pressures ranging from 0.5 to 1.5 bar and temperatures of 293 and 303 K. These membranes showed a promising performance, reaching values of propylene permeability up to 1800 Barrer and very high propylene/propane selectivities. The reported model constitutes a very useful tool for process optimisation and scale-up.

Keywords

Propylene, propane, $AgBF_4$, PVDF-HFP, membrane, fixed-site carrier mathematical model.

1. Introduction

The global production of ethylene and propylene exceeds 200 million tones per year, being the purification stage responsible for 0.3% of the global energy use [1]. Current separation processes, mainly cryogenic distillation, consist on highly energy and capital intensive operations [2], which typically account for 45-55% of industrial processes energy consumption [1]. Some alternative processes to cryogenic distillation have been proposed over the last times, being the most studied: extractive distillation [3], physical adsorption on molecular sieves [4], and chemical adsorption [5]. Nonetheless, some problems as low olefin loads and complicated regeneration cycles have prevent these alternatives from replacing traditional distillation [6].

Recently, membrane technology has emerged as a possible solution that allows process intensification [7], which will lead to energy and capital savings in many gas separation processes, such as CO_2 capture [8], CO separation [9], natural gas purification [10] and hydrogen production [11]. In the short term, membranes can be used for bulk separation, using distillation for the final "refining" of the product. Such hybrid systems would reduce the energy requirements of olefin production by a factor of two or three [1]. A wide range of membrane compositions have been reported for olefin/paraffin separation, including liquid, polymeric and inorganic membranes [12-16]. However, these technologies face some major drawbacks. Liquid membranes show a serious lack of stability due to solvent evaporation [17]. Polymeric dense membranes suffer from poor performance in terms of selectivity and permeability due to the similar sizes of permeant species [18]. Lastly, inorganic membranes usually require complex and expensive preparation methods and show low mechanical resistance.

The development of new materials has promoted recent studies on their application to gas separation. In this regard, new studies assess the performance of nanocomposite membranes [19], mixed-matrix membranes containing metal organic frameworks (MOFs) [20-22], polymers with intrinsic microporosity (PIMs) [23] and membranes containing metallic nanoparticles [24], achieving high olefin/paraffin selectivities.

Among the membrane systems reported, those regarding the facilitated transport of olefins using a transition metal cation as carrier agent have shown great performance for olefin/paraffin separations [25-27]. The main advantage of carrier mediated facilitated transport membranes is their capability to achieve high values of selectivity and permeability at the same time, thus overcoming the existing tradeoff between these two variables [28,29]. Facilitated transport membranes for olefin/paraffin separation are prepared dissolving a silver salt within a polymeric matrix, forming a solid membrane, usually known as polymer electrolyte. On this matter, Bai et al. [30] synthesized ethyl-cellulose membranes modified with the incorporation of several metal-ions, achieving higher selectivity when testing silver cations instead of other transition metals. Kim et al. [31] tested EPR-coated polyester membranes with physically dispersed silver aggregates that dissolved in situ when in contact with the olefin, resulting in high selectivity towards the olefin; in addition, polymerized ionic liquids have been also assessed as a matrix for the incorporation of silver cations with promising results [32]. These membranes make use of the silver cations ability to selectively and reversibly coordinate with olefin molecules, following a π–bond complexation mechanism [33,34]. Additionally, our research group has developed composite membranes incorporating ionic liquids to the matrix polymer in order to improve the separation performance and stabilizing the silver cations in the membrane [28,35].

In this work, the use of dense polymeric facilitated transport membranes made of PVDF-HFP fluoropolymer and $AgBF_4$ silver salt is reported. When $AgBF_4$ dissolves into the polymer, it dissociates into Ag^+ and BF_4^- -ions. Then, Ag^+ ions tend to bond with those polymer atoms that can donate electrons to stabilize silver cations. Previous experimental studies have widely proven this distribution of cations, assessing their interactions with electron donor atoms of the polymer by means of FTIR spectra [36,37]. Once the membrane is in contact with the olefin, π-bonding complexation between the olefin and the cation takes place. Finally, due to the partial pressure gradient, the olefin follows a hopping movement from one fixed cation to the next, giving place to fixed carrier transport mechanism [38,39]. PVDF-HFP fluoropolymer was selected because of its well-known chemical, mechanical and thermal stability and its good miscibility with $AgBF_4$ silver salt; furthermore, besides the copolymerization with HFP decreases its crystallinity degree to around 0.3 [40], certain crystallinity in the polymer structure may reduce the paraffin sorption, while the olefin solubility remains high due to its complexation with the silver cations, increasing the selectivity of the membrane.

Previously, interesting works have been reported trying to describe this facilitated transport phenomenon in similar systems. In this regard, Smith and Quinn [41] studied the facilitated transport of carbon monoxide through cuprous chloride solutions; Ravanchi et al. [42] and Kasahara et al. [43] developed mathematical models for propane/propylene separation using supported liquid membranes and ion-gel membranes composed of gelled ionic liquids on PTFE supports, respectively.

The present work proposes a novel mathematical description for propylene flux through solid PVDF-HFP/Ag^+ facilitated transport membranes. Although previous reports of this research group have assessed the addition of ionic liquids as additives to

promote carrier mobility [28], its use has been avoided in this study in order to limit the transport mechanisms to fixed site carrier and solution-diffusion. The mathematical approach at this stage involves the experimental determination of the activation energy (Ea), the equilibrium constant (Kp) and the influence of silver concentration (β), whereas the fitting parameter (α) has been estimated using Aspen Custom Modeler software. The model is able to describe the influence of the main operating variables on propylene flux, such as temperature, partial pressure and membrane composition. This model is the necessary tool for future process design, scale-up and optimization.

2. Experimental

2.1 Chemicals

Propylene and propane gases were purchased from Praxair with a purity of 99.5% for both gases. Poly(vinylidene fluoride-co-hexafluoropropylene) (PVDF-HFP) was supplied by Sigma Aldrich. Silver tetrafluoroborate ($AgBF_4$) with a minimum purity of 99% was purchased from Apollo Scientific Ltd. Tetrahydrofuran (THF) was used as solvent for membrane synthesis. All chemicals were used as received with no further purification.

2.2 Membrane synthesis

PVDF-HFP/$AgBF_4$ membranes were synthesized using the solvent casting method. The selected amount of PVDF-HFP is dissolved in 10 mL of THF by stirring in a sealed glass vial to prevent solvent evaporation. After 24 hours of stirring at room temperature, the vial is heated at 50 ºC during 5 minutes until the polymer is completely dissolved. Once the polymeric solution is prepared, it is mixed with the desired amount of silver salt and stirred for 10 min. Finally, the membrane precursor is poured in a Petri dish and located in a vacuum oven for 24 hours at 25 ºC and 300 mbar under dark conditions. The resulting thickness of the prepared dense films depends on the silver load, but in all cases, it is around 60±10 μm. For calculation purposes, the real thickness of each membrane has been considered, being measured using a digital micrometer Mitutoyo Digimatic MDC-25SX (accuracy ± 0.001 mm).

2.3 Membrane morphology characterization

The cross-section and surface morphology of the membranes were observed using scanning electron microscopy (Carl Zeiss EVO MA 15). The samples were prepared by immersing and fracturing the membranes in liquid nitrogen followed by gold sputtering

using a Balzers Union SCD040 sputter coating system. The line-scan spectrum of energy dispersive X-ray spectroscopy (EDX) was applied to the same samples of SEM to determine the silver distribution profile in the membrane cross-section.

2.4 Gas permeation experiments

The permeation experiments were conducted using the gas mixture continuous flow technique detailed elsewhere [28]; briefly, the membrane is placed in a permeation cell and the gas mixture is continuously fed into the upper chamber. Nitrogen gas is used in the lower chamber as sweeping gas. The retentate and permeate streams are finally analyzed using gas chromatography and the experimental propylene flux is calculated by a simple mass balance, as shown in Equation 1.

$$J_{C_3H_6} = \frac{1}{A}\frac{x_{C_3H_6}}{x_{N_2}} F_{N_2} \quad (1)$$

Where A is the effective membrane area, $x_{C_3H_6}$ and x_{N_2} are the propylene and nitrogen mole fractions, respectively, in the permeate chamber outlet stream and F_{N_2} is the nitrogen molar flow rate. Gas permeation experiments were carried out at the experimental conditions displayed in Table 1.

Table 1. Experimental conditions

Experimental condition	Value
T (K)	293-313
Permeation area (cm^2)	53
N_2 flow (mL min^{-1})	20
C_3H_6 flow (mL min^{-1})	10
C_3H_8 flow (mL min^{-1})	10
Feed side pressure (bar)	1-4
Permeate side pressure (bar)	1

In order to assess the influence of silver concentration a set of three membranes with different silver loads were synthesized; membrane composition is shown in Table 2.

Table 2. Membrane set

Membrane	$AgBF_4$ load (% w/w)	Thickness (μm)	[Ag] ($mol \cdot L^{-1}$)
1	16.7	53	2.47
2	28.6	67	3.91
3	37.5	71	5.53

3. Mathematical modeling

The transport of propylene through the membrane is the result of two different transport mechanisms acting simultaneously, as illustrated in Figure 1.

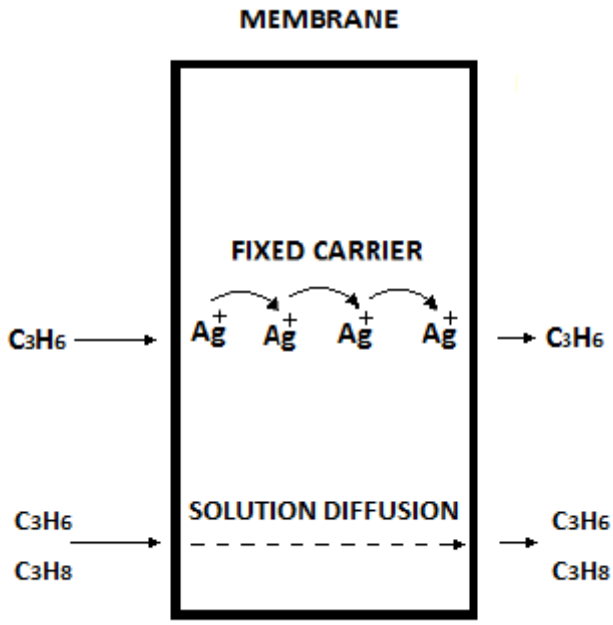

Figure 1. Transport mechanisms acting within the membrane.

When a gas bulk is in contact with a non-porous material, gas molecules start to solubilize spontaneously in the polymer matrix. Adsorbed molecules then diffuse through the membrane, resulting in a net gas flux if a partial pressure gradient is applied. Furthermore, when a certain quantity of $AgBF_4$ is added to the membrane, it dissociates into its ions. Silver cations tend to form new bonds with those atoms present in the polymer matrix that can donate their electrons to stabilize Ag^+. These fixed silver cations promote the fixed carrier mechanism [44]. If the membrane is exposed to olefins, complexation takes place between the olefin molecules and the Ag^+ cations that are partially coordinated with the polymer matrix [45]. The olefin then follows a

hopping mechanism until it reaches the other side of the membrane, where the olefin is released. The chemical reaction between the olefin and the silver cation is described as:

$$Ag^{+} + C_3H_6 \overset{Keq}{\leftrightarrow} Ag^{+}(C_3H_6) \quad (2a)$$

In the heterogeneous form:

$$\left[Ag^{+}\right] + P_{C_3H_6} \overset{Kp}{\leftrightarrow} \left[Ag^{+}\left(C_3H_6\right)\right] \quad (2b)$$

The olefin flux given by the joint action of the two transport mechanisms can be expressed by Equation 3 [46]:

$$J_{C_3H_6} = -D_{C_3H_6,m}\frac{dC_{C_3H_6}}{dx} - A\frac{dC_{C_3H_6}}{dx} \quad (3)$$

where the parameter A acts as an effective diffusivity in the fixed site carrier transport. Integrating Equation 3 in the membrane domain results in Equation 4:

$$J_{C_3H_6} = D_{C_3H_6,m}\frac{C^0_{C_3H_6} - C^L_{C_3H_6}}{L} + A\frac{C^0_{C_3H_6} - C^L_{C_3H_6}}{L} \quad (4)$$

Assuming a sorption equilibrium at the interface:

$$J_{C_3H_6} = D_{C_3H_6,m}\cdot S_{C_3H_6,m}\frac{p^0_{C_3H_6} - p^L_{C_3H_6}}{L} + K_H\frac{p^0_{C_3H_6} - p^L_{C_3H_6}}{L} \quad (5)$$

Where K_H acts as an effective permeability or "hopping constant" for the olefin through the reactive pathway. The values of diffusivity (D) and solubility (S) of propylene in the PVDF-HFP matrix have been calculated in previous works [35]; however, in this case, the contribution of the solution diffusion mechanism can be neglected compared with the fixed carrier contribution. The transport capability of the

fixed site carrier mechanism is a function of the membrane silver loading and the temperature [38]. A mathematical expression can be derived for the dependence of K_H with temperature and silver concentration, as shown in Equation 6.

$$K_H = \alpha \left(\frac{[Ag^T]}{1 + K_P \cdot p^0_{C_3H_6}} \right)^{\beta} e^{\frac{Ea}{R}\left(\frac{1}{293} - \frac{1}{T}\right)} \quad (6)$$

The effect of temperature is given by an Arrhenius type expression, while the term in brackets is the concentration of uncomplexed silver cations, as obtained from the chemical equilibrium. The exponent β was introduced to correct the silver concentration influence on the propylene flux, given the percolation threshold observed in these membranes by several authors [47-49]. The parameter α is the fitting parameter of the model.

On the other hand, given that propane is only affected by fickian diffusion, its flux can be easily described by the solution-diffusion equation:

$$J_{C_3H_8} = D_{C_3H_8,m} \cdot S_{C_3H_8,m} \frac{p^0_{C_3H_8} - p^L_{C_3H_8}}{L} \quad (7)$$

4. Results and discussion

4.1 Membrane morphology

Figure 2 displays the SEM photographs of a PVDF-HFP membrane and PVDF-HFP/$AgBF_4$ membranes **1** and **3**. In all cases the PVDF-HFP forms a homogeneous dense polymeric matrix with no signs of porosity or differentiated layers. Furthermore, no particle clusters appear in the polymer electrolyte membranes, indicating that the added salt is completely dissolved.

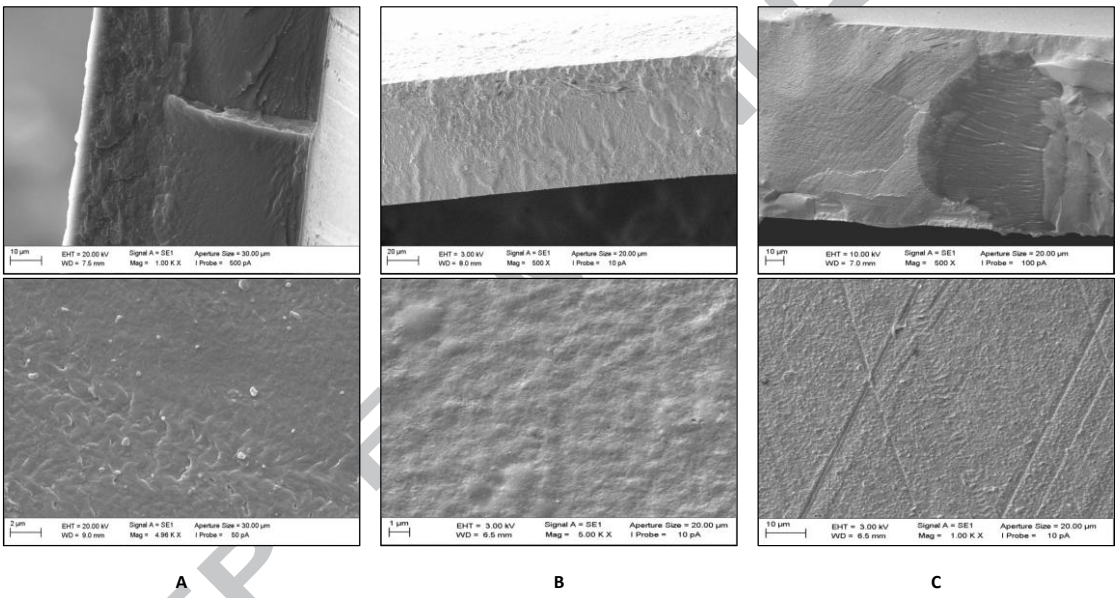

*Figure 2. Cross-section and surface morphology of: A) Pure PVDF-HFP membrane, B) membrane **1** [Ag]=2.47 M, C) membrane **3** [Ag]=5.53 M.*

The EDX spectra of the membrane with the highest silver loading displayed in Figure 3 shows a uniform distribution of the element silver along the cross-section of the membrane, with no evidence of silver particles formation. This is in good agreement with the previously discussed works on the interactions between the Ag^+ cations and the polymer matrix [36,37].

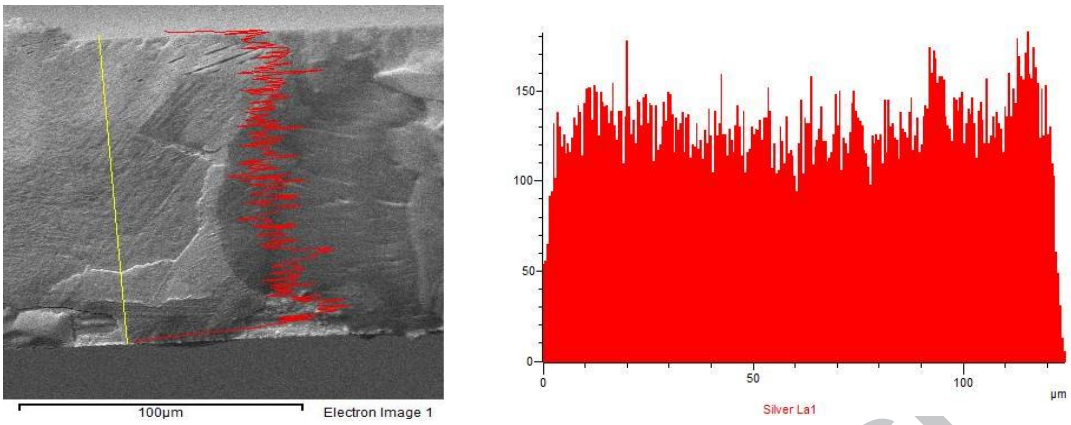

*Figure 3. SEM-EDX scan-line and silver distribution profile in the cross-section of membrane **3** [Ag]=5.53 M.*

4.2 Permeation results

In this section, the permeation results are discussed; the experimental propylene flux through the membranes **1-3** as a function of propylene partial pressure is depicted in Figure 4 at 293 and 303 K, respectively.

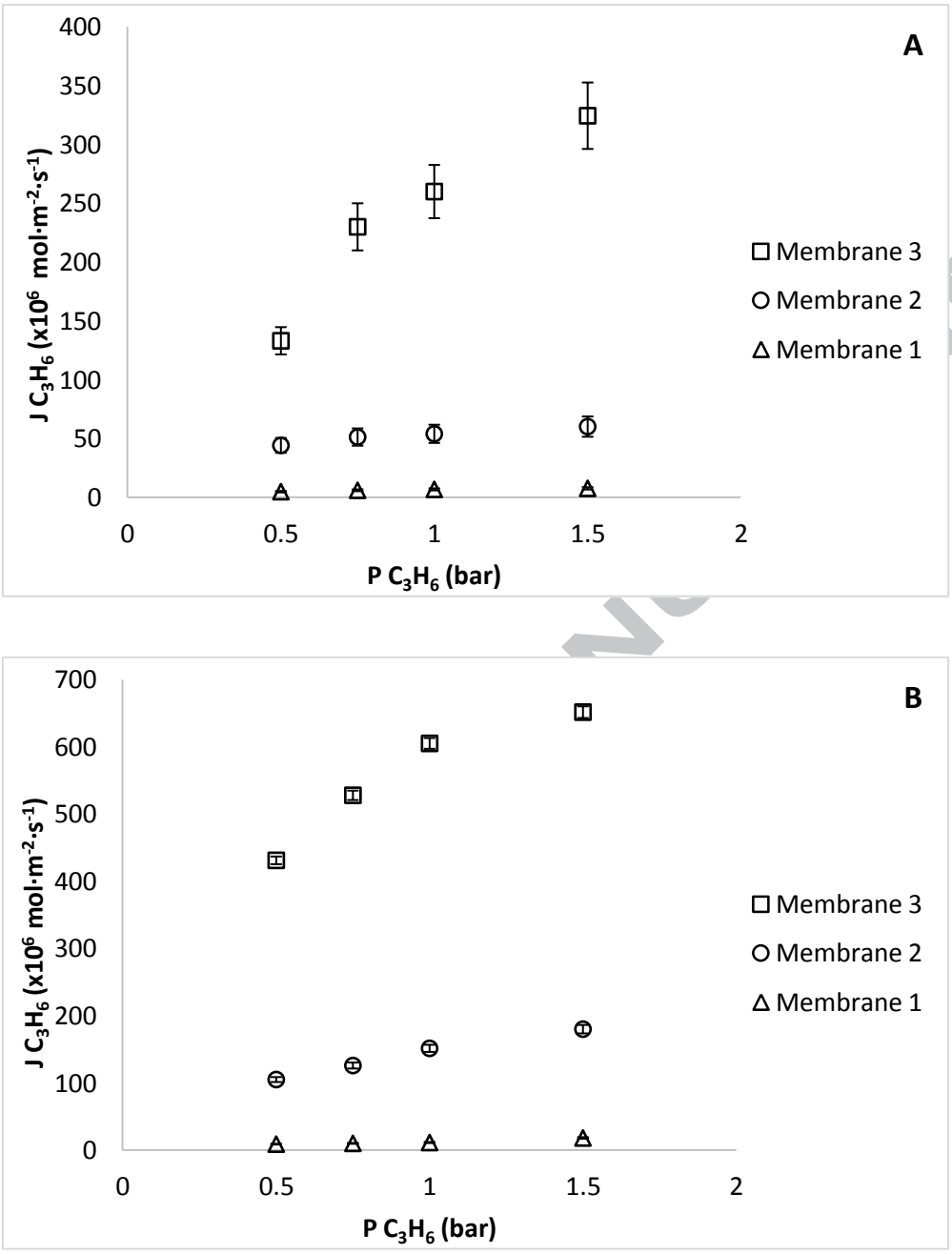

*Figure 4. Propylene flux at (a) 293 and (b) 303 K as a function of the feed partial pressure in membrane **1** [Ag]=2.47 M, membrane **2** [Ag]=3.91 M and membrane **3** [Ag]=5.53 M.*

As the difference of propylene partial pressure is the driving force in the permeation process, the olefin flux increases when its feed partial pressure rises. In contrast to the conventional solution-diffusion transport mechanism, that describes a linear increase of the permeate flux with increasing driving force, i.e. partial pressure difference, these membranes display the characteristic fixed-site-carrier facilitated transport profile

described elsewhere [50]. At very low values of the driving force, most part of the transported molecules follow the complexing mechanism, resulting in a non-linear profile. On the other hand, for high driving forces, every silver cation is bound to propylene molecules and the carrier becomes saturated. In this state, any flux increase is mainly induced by the solution-diffusion mechanism, and thus, the linear trend is only achieved after surpassing a threshold value of the partial pressure gradient.

Comparing Figures 4 (a) and (b) it can be observed that the temperature has a strong influence on the permeation process, increasing the flux of propylene. This increase of the olefin flux is due to the enhancement in the gas diffusivity, as reported before [35]. The temperature also has a positive influence on the rate of complexation and decomplexation reactions, thus enhancing the olefin facilitated transport. In contrast to diffusivity, the solubility of both gases slightly decreases with temperature; nonetheless, the influence of this trend is completely overlapped by the diffusivity effect. However, as the paraffin diffusivity undergoes an increasing trend with temperature, it results in a selectivity decrease towards the olefin at higher temperatures.

Pristine PVDF-HFP copolymer is known for being a low permeable material. This property combined with transport facilitation towards propylene yields very high selectivity. In fact, the propane concentration in the permeate stream when testing membranes **1** and **2** was below the gas chromatograph detection limit (0.025 vol.%). The permeate stream of membrane **3** contained a minor quantity of propane at the higher feed pressures, as displayed in Figure 5. The resulting selectivity ranges from 100 to 300. Given that previous studies involving pure gases report lower values of propane permeability in PVDF-HFP [35], a dragging effect caused by the high propylene fluxes is probably happening in membrane **3**, resulting in a propane

permeability increase. Figure 5 shows the difference between the experimental fluxes of propylene and propane.

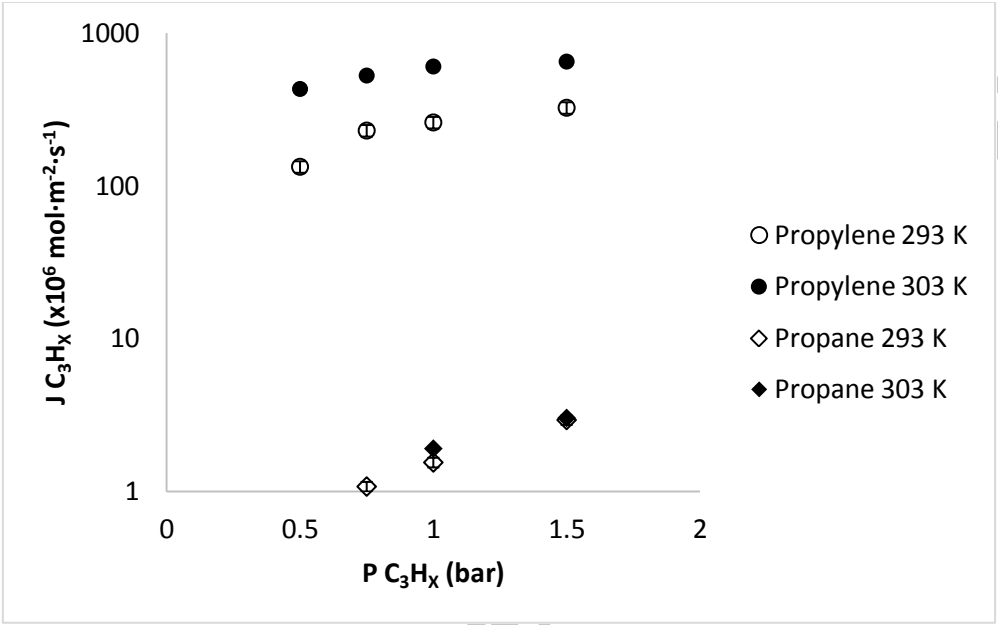

*Figure 5. Experimental fluxes of propylene and propane in membrane **3** at 293 and 303 K, at different partial pressure.*

Thus, these experimental results demonstrate that it is possible to achieve high propylene flux and selectivity even at low partial pressures and moderate temperatures.

Comparing all three membranes in terms of silver loading and propylene flux, one can observe that the silver concentration has a major influence on the olefin permeability. When the silver content increases within the membrane, more silver cations are available to coordinate with olefin molecules. The result is a noticeable increase in propylene facilitated transport that follows an exponential trend, Figure 6. A similar behaviour was reported by Yoon et al. [47] in PEOx and PVP with $AgBF_4$ and $AgCF_3SO_3$ silver salts, by Morisato et al. [48] in PA-12-PTMO/$AgBF_4$ membranes, and by Kim et al. [49] in different polymer/silver membranes, although it has not been previously reported in PVDF-HFP fluoropolymer. This trend evidences a percolation

threshold; at low carrier concentrations, the facilitated transport is almost negligible, while increasing the concentration results in a major increase of the olefin flux. This phenomenon is related to the proximity between active sites; at low concentrations, the distance between two consecutive cations is too large to allow the facilitated transport; on the other hand, at higher concentrations the silver cations are close enough to transport the olefin. In these membranes, the percolation threshold seems to be surpassed at silver concentrations higher than 2.5 $mol \cdot L^{-1}$.

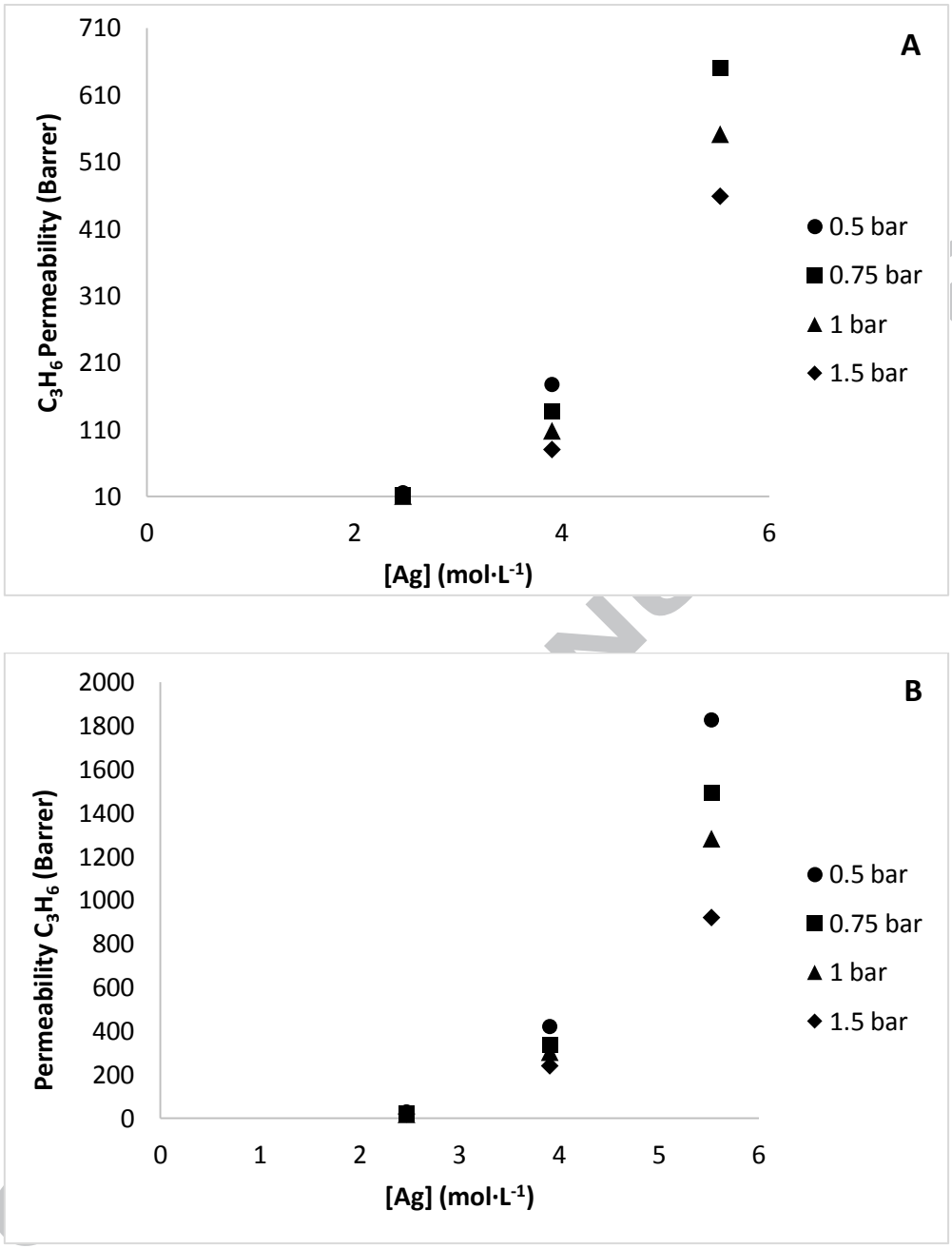

Figure 6. Permeability of propylene with increasing silver concentration at (a) 293 and (b) 303 K.

4.3 Mathematical Model

One of the main targets of this work is to provide a simple yet effective model to predict the olefin flux in this polymer/silver system. This tool will be useful to design

and optimize commercial attractive configurations as spiral wound or hollow fiber geometries. The model contains one fitting parameter and three calculated parameters.

In order to avoid interferences in parametric sensitivity, the experimental determination of the activation energy, the equilibrium constant and the exponent β has been carried out isolating the influence of temperature from the influence of silver concentration. The values of calculated parameters are shown in Table 3.

Table 3. Calculated model parameters.

Parameter	Value
Activation energy, Ea (kJ mol^{-1})	61
Equilibrium constant, K_p (bar^{-1})	0.12
Beta exponent, β	4.235

To calculate the activation energy of the permeation process, experimental data at constant pressure and constant silver concentration, modifying the temperature, were fitted to an Arrhenius type equation, Equation 8:

$$\ln K_H = \ln \alpha' + \frac{Ea}{R}\left[\frac{1}{T_{ref}} - \frac{1}{T}\right] \quad (8)$$

Using the same methodology, the equilibrium constant K_P and the exponent β were determined by regression of permeability data at constant temperature, with silver concentration and olefin partial pressure, Equation 9:

$$K_H = \alpha''\left(\frac{Ag}{1+K_p \cdot p_i}\right)^{\beta} \quad (9)$$

Aspen Custom Modeler software was used to fit the experimental data to the model equations and estimate the fitting parameter α, which has a value of $3.24x10^{-11}$ for this particular case study.

Once the model parameters are determined, the model describes the permeation process of propylene through the facilitated transport membrane, providing that all operating variables are inside the studied range. Figure 7 shows experimental and model flux values of propylene at several temperatures and olefin partial pressures with membranes **1** to **3**.

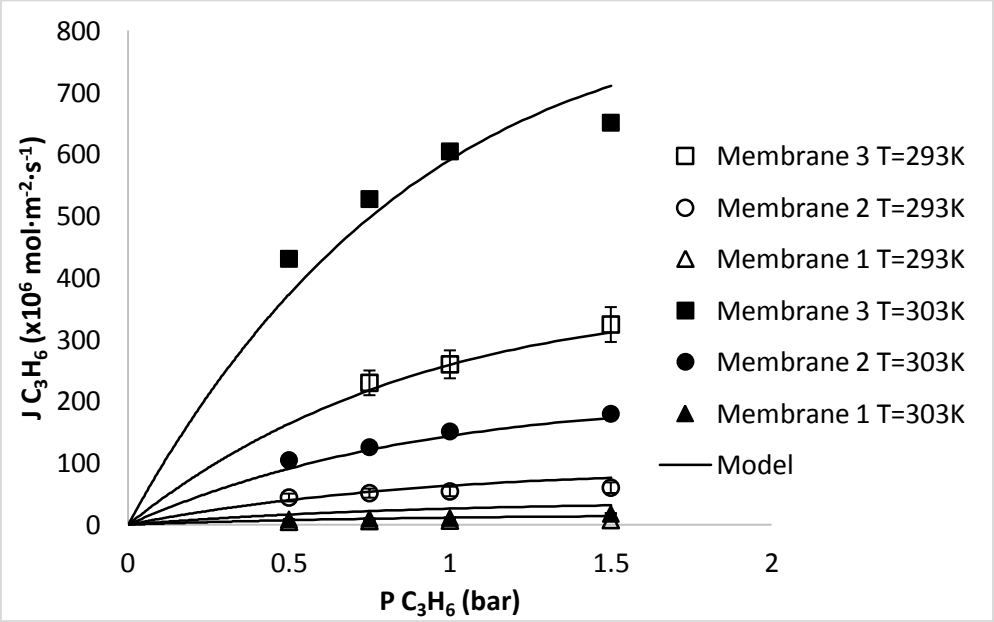

*Figure 7. Propylene experimental flux and model prediction for the membranes **1** to **3** at 293 and 303 K, and at different feed partial pressures.*

The estimated propylene fluxes are represented against the experimental propylene fluxes in the parity graph shown in Figure 8. In the parity graph, a 15% error range is also displayed, proving that the majority of points fall within this range, and checking the adequacy of the proposed model to describe the experimental behavior of propane/propylene separation using PVDF-HFP/Ag^+ membranes.

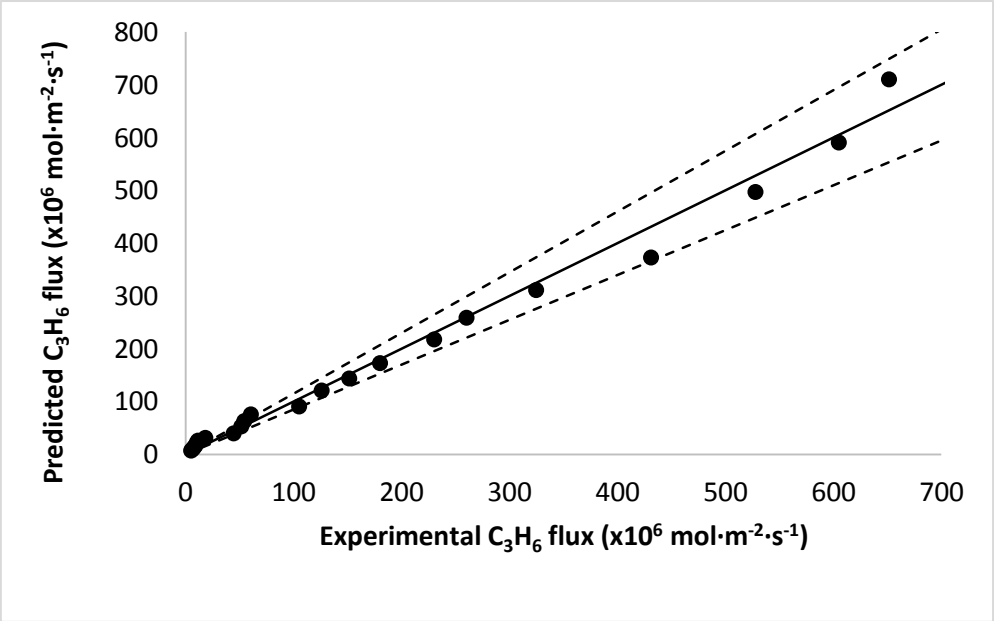

Figure 8. Model parity graph with a 15% error range.

4.4 Membranes comparison

Various polymer electrolytes comprising different polymer matrices and silver salts have been previously reported for propylene/propane separation. Table 4 displays the selectivity values achieved by other authors when similar propylene/propane gas mixtures were tested. It is remarkable the performance of the PDMS/$AgBF_4$ membranes reported by Kim et al. [51]; with the particularity that the silver cations are not bounded to the polymer chains, according to the authors; silver remains forming ionic aggregates that progressively dissolve upon its contact with the olefin. The use of PVDF-HFP as polymeric matrix reported in this work yields higher selectivity compared with other membranes that use the same silver salt, and shows great potential for the intensification of the olefin/paraffin separation process.

Table 4. Comparison with previous reported facilitated transport membranes.

Membrane	C_3H_6/C_3H_8 gas mixture	Feed pressure (bar)	Thickness (μm)	Permeance (GPU) [a]	Selectivity	Ref.
Poly(ethylene-co-propylene) / 62 wt.% $AgBF_4$	50/50		1-2	7	55	[31]
PEBAX 1657 / 50 wt.% $AgBF_4$	50/50	4	25	4[b]	17.2	[27]
PEBAX 1657 / 50 wt.% $AgBF_4$	66/34	2	25	5[b]	20.2	[27]
PEOx/$AgBF_4$ [Ag]/[C=O] 1:1	50/50	2.76	1	35	58	[47]
PEOx/$AgCF_3SO_3$ [Ag]/[C=O] 1:1	50/50	2.76	1	32	19	[47]
PVP/$AgBF_4$ [Ag]/[C=O] 1:1	50/50	2.76	1	36	65	[47]
PVP/$AgCF_3SO_3$ [Ag]/[C=O] 1:1	50/50	2.76	1	28	18	[47]
PDMS/57 wt.% $AgBF_4$	50/50		2	13	150	[51]
PVDF-HFP/60 wt.% $AgBF_4$	50/50	2	71	25[b]	300	This work

[a] Permeance in GPU. 1 GPU=1x10^{-6} cm^3 (STP)/cm^2 s cmHg.

[b] Calculated from reported permeability and thickness.

5. Conclusions

A mathematical expression for the "effective permeability" of propylene by the fixed carrier mechanism has been deduced and the fitting parameter has been estimated based on experimental data. The validity of the model has been checked by comparing simulated and experimental permeation data for propylene/propane gas mixtures in PVDF-HFP/Ag^{+}.

The resulting olefin fluxes follow the characteristic trend of facilitated transport processes when increasing the feed pressure, and indicate a promising performance in terms of propylene permeability. The silver loading dramatically increases the propylene flux in an exponential trend, which suggests the existence of a concentration threshold. The comparison between experimental and predicted values and the model parity graph suggest a reliable goodness of fit.

The mathematical approach reported in this work is susceptible to be applied in those membrane systems where the fixed carrier mechanism is present and allows to calculate its contribution to the total permeate flux in a fast and simple manner. Therefore, this model will be a valuable tool for future design and optimization of more complex propylene/propane separation systems (i.e. mobile-fixed carrier hybrid membranes) in more efficient process configurations.

Acknowledgement

Financial support from the Spanish Ministry of Science under the projects CTQ2015-66078-R and CTQ2016-75158-R (MINECO, Spain-FEDER 2014–2020) is gratefully acknowledged. Raúl Zarca also thanks the Universidad de Cantabria for a postgraduate fellowship.

Nomenclature

A membrane effective area [m^2]

C concentration [mol L^{-1}]

D diffusion coefficient [m^2 s^{-1}]

Ea activation energy [kJ mol^{-1}]

F molar flowrate [mol s^{-1}]

J molar flux [mol m^{-2} s^{-1}]

K_{eq} equilibrium constant [m^3 mol^{-1}]

K_H fixed carrier effective permeability [mol bar^{-1} m^{-1} s^{-1}]

K_p heterogeneous equilibrium constant [bar^{-1}]

L membrane thickness [m^3 mol^{-1} s^{-1}]

p pressure [bar]

R universal gas constant [8.314 J mol^{-1} K^{-1}]

S gas solubility [mol bar^{-1} m^{-3}]

T temperature [K]

x mole fraction [-]

Greek letter

α fitting parameter

β percolation threshold exponent [-]

Superscript / subscript

0 feed side

C_3H_6 propylene

C_3H_8 propane

L permeate side

N_2 nitrogen

m membrane

ref reference

References

[1] D.S. Sholl, R.P. Lively, Seven chemical separations to change the world, Nature 532 (2016) 435-437.

[2] J.L. Humphrey, A.F. Seibert, R.A. Koort, Separation technologies: Advances and priorities, U.S. Department of Energy Report No. DOE/ID/12920-1 (1991).

[3] R. Kumar, J.M. Prausnitz, C.J. King, Process design considerations for extractive distillation: separation of propylene-propane, in: D. Tassios (Ed.), Extractive and azeotropic distillation, American Chemical Society, Washington D.C., 1974, pp. 16-34.

[4] C.M. Shu, S. Kulvaranon, M.E. Findley, A.I. Liapis, Experimental and computational studies on propane-propylene separation by adsorption and variable-temperature stepwise desorption, Sep. Technol. 1 (1990) 18-28.

[5] R.T. Yang, Adsorbents : fundamentals and applications, John Wiley & Sons, Hoboken, NJ, 2003, pp. 191-230.

[6] R.B. Eldridge, Olefin/paraffin separation technology: A review, Ind. Eng. Chem. Res. 32 (1993) 2208-2212.

[7] J. Charpentier, In the frame of globalization and sustainability, process intensification, a path to the future of chemical and process engineering (molecules into money), Chem. Eng. J. 134 (2007) 84-92.

[8] T.C. Merkel, X. Wei, Z. He, L.S. White, J.G. Wijmans, R.W. Baker, Selective exhaust gas recycle with membranes for CO_2 capture from natural gas combined cycle power plants, Ind. Eng. Chem. Res. 52 (2013) 1150-1159.

[9] G. Zarca, W.J. Horne, I. Ortiz, A. Urtiaga, J.E. Bara, Synthesis and gas separation properties of poly(ionic liquid)-ionic liquid composite membranes containing a copper salt, J. Membr. Sci. 515 (2016) 109-114.

[10] M. Askari, T. Chung, Natural gas purification and olefin/paraffin separation using thermal cross-linkable co-polyimide/ZIF-8 mixed matrix membranes, J. Membr. Sci. 444 (2013) 173-183.

[11] R. Swaidan, B. Ghanem, I. Pinnau, Fine-tuned intrinsically ultramicroporous polymers redefine the permeability/selectivity upper bounds of membrane-based air and hydrogen separations, ACS Macro Lett. 4 (2015) 947-951.

[12] J. Caro, M. Noack, P. Kölsch, R. Schäfer, Zeolite membranes - state of their development and perspective, Microporous Mesoporous Mater. 38 (2000) 3-24.

[13] Y.S. Lin, I. Kumakiri, B.N. Nair, H. Alsyouri, Microporous inorganic membranes, Sep. Purif. Methods. 31 (2002) 229-379.

[14] M. Fallanza, A. Ortiz, D. Gorri, I. Ortiz, Experimental study of the separation of propane/propylene mixtures by supported ionic liquid membranes containing Ag+–RTILs as carrier, Sep. Purif. Technol. 97 (2012) 83-89.

[15] S. Najari, S.S. Hosseini, M. Omidkhah, N.R. Tan, Phenomenological modeling and analysis of gas transport in polyimide membranes for propylene/propane separation, RSC Adv. 5 (2015) 47199-47215.

[16] K.-S. Liao, J.-Y. Lai, T.-S. Chung, Metal ion modified PIM-1 and its application for propylene/propane separation, J. Membr. Sci. 515 (2016) 36-44.

[17] M. Teramoto, H. Matsuyama, T. Yamashiro, Y. Katayama, Separation of ethylene from ethane by supported liquid membranes containing silver-nitrate as a carrier, J. Chem. Eng. Japan. 19 (1986) 419-424.

[18] R. Faiz, K. Li, Polymeric membranes for light olefin/paraffin separation, Desalination 287 (2012) 82-97.

[19] H. Sun, B. Yuan, P. Li, T. Wang, Y. Xu, Preparation of nanoporous graphene and the application of its nanocomposite membrane in propylene/propane separation, Funct. Mater. Lett. 08 (2015) 1550019.

[20] U. Böhme, B. Barth, C. Paula, A. Kuhnt, W. Schwieger, A. Mundstock, J. Caro, M. Hartmann, Ethene/ethane and propene/propane separation via the olefin and paraffin selective metal-organic framework adsorbents CPO-27 and ZIF-8, Langmuir. 29 (2013) 8592-8600.

[21] G. Chang, M. Huang, Y. Su, H. Xing, B. Su, Z. Zhang, Q. Yang, Y. Yang, et al., Immobilization of Ag(I) into a metal-organic framework with -SO3H sites for highly selective olefin-paraffin separation at room temperature, Chem. Commun. 51 (2015) 2859-2862.

[22] H.T. Kwon, H. Jeong, Improving propylene/propane separation performance of Zeolitic-Imidazolate framework ZIF-8 Membranes, Chem. Eng. Sci. 124 (2015) 20-26.

[23] R.J. Swaidan, X. Ma, E. Litwiller, I. Pinnau, Enhanced propylene/propane separation by thermal annealing of an intrinsically microporous hydroxyl-functionalized polyimide membrane, J. Membr. Sci. 495 (2015) 235-241.

[24] C.G.F. Rezende, C.P. Borges, A.C. Habert, Sorption of propylene and propane in polyurethane membranes containing silver nanoparticles, J Appl Polym Sci. 133 (2016).

[25] J.H. Kim, B.R. Min, J. Won, S.H. Joo, H.S. Kim, Y.S. Kang, Role of polymer matrix in polymer/silver complexes for structure, interactions, and facilitated olefin transport, Macromolecules. 36 (2003) 6183-6188.

[26] J.H. Kim, B.R. Min, J. Won, Y.S. Kang, Revelation of facilitated olefin transport through silver-polymer complex membranes using anion complexation, Macromolecules 36 (2003) 4577-4581.

[27] R. Surya Murali, K. Yamuna Rani, T. Sankarshana, A.F. Ismail, S. Sridhar, Separation of binary mixtures of propylene and propane by facilitated transport through silver incorporated poly(ether-block-amide) membranes, Oil Gas Sci. Technol. 70 (2015) 381-390.

[28] M. Fallanza, A. Ortiz, D. Gorri, I. Ortiz, Polymer-ionic liquid composite membranes for propane/propylene separation by facilitated transport, J. Membr. Sci. 444 (2013) 164-172.

[29] L. Liu, X. Feng, A. Chakma, Unusual behavior of poly(ethylene oxide)/$AgBF_4$ polymer electrolyte membranes for olefin–paraffin separation, Sep. Purif. Technol. 38 (2004) 255-263.

[30] S. Bai, S. Sridhar, A.A. Khan, Recovery of propylene from refinery off-gas using metal incorporated ethylcellulose membranes, J. Membr. Sci. 174 (2000) 67-79.

[31] J.H. Kim, B.R. Min, Y.W. Kim, S.W. Kang, J. Won, Y.S. Kang, Novel composite membranes comprising silver salts physically dispersed in poly(ethylene-co-propylene) for the separation of propylene/propane, Macromol. Res. 15 (2007) 343-347.

[32] L.C. Tomé, D. Mecerreyes, C.S.R. Freire, L.P.N. Rebelo, I.M. Marrucho, Polymeric ionic liquid membranes containing IL-Ag^+ for ethylene/ethane separation via olefin-facilitated transport, J. Mater. Chem. A. 2 (2014) 5631-5639.

[33] J.S. Dewar, A review of the pi-complex theory, Bull. Soc. Chim. Fr. 18 (1951) C71-C79.

[34] L.M. Galán Sánchez, G.W. Meindersma, A.B. Haan, Potential of silver-based room-temperature ionic liquids for ethylene/ethane separation, Ind. Eng. Chem. Res. 48 (2009) 10650-10656.

[35] R. Zarca, A. Ortiz, D. Gorri, I. Ortiz, Facilitated transport of propylene through composite polymer-ionic liquid membranes. Mass transfer analysis, Chem. Prod. Process Model. 11 (2016) 77-81.

[36] J. Chang, S.W. Kang, CO_2 separation through poly(vinylidene fluoride-co-hexafluoropropylene) membrane by selective ion channel formed by tetrafluoroboric acid, Chem. Eng. J. 306 (2016) 1189-1192.

[37] S. Sunderrajan, B.D. Freeman, C.K. Hall, I. Pinnau, Propane and propylene sorption in solid polymer electrolytes based on poly(ethylene oxide) and silver salts, J. Membr. Sci. 182 (2001) 1-12.

[38] E.L. Cussler, R. Aris, A. Bhown, On the limits of facilitated diffusion, J. Membr. Sci. 43 (1989) 149-164.

[39] R.D. Noble, Analysis of facilitated transport with fixed site carrier membranes, J. Membr. Sci. 50 (1990) 207-214.

[40] S. Abbrent, J. Plestil, D. Hlavata, J. Lindgren, J. Tegenfeldt, Å. Wendsjö, Crystallinity and morphology of PVdF-HFP-based gel electrolytes, Polymer 42 (2001) 1407-1416.

[41] D.R. Smith, J.A. Quinn, The facilitated transport of carbon monoxide through cuprous chloride solutions, AIChE J. 26 (1980) 112-120.

[42] M.T. Ravanchi, T. Kaghazchi, A. Kargari, Facilitated transport separation of propylene-propane: Experimental and modeling study, Chem. Eng. Process. 49 (2010) 235-244.

[43] S. Kasahara, E. Kamio, R. Minami, H. Matsuyama, A facilitated transport ion-gel membrane for propylene/propane separation using silver ion as a carrier, J. Membr. Sci. 431 (2013) 121-130.

[44] R. Faiz, K. Li, Olefin/paraffin separation using membrane based facilitated transport/chemical absorption techniques, Chem. Eng. Sci. 73 (2012) 261-284.

[45] A. Ortiz, L.M. Galán Sanchez, D. Gorri, A.B. De Haan, I. Ortiz, Reactive ionic liquid media for the separation of propylene/propane gaseous mixtures, Ind. Eng. Chem. Res. 49 (2010) 7227-7233.

[46] R.D. Noble, Generalized microscopic mechanism of facilitated transport in fixed site carrier membranes, J. Membr. Sci. 75 (1992) 121-129.

[47] Y. Yoon, J. Won, Y.S. Kang, Polymer electrolyte membranes containing silver ion for facilitated olefin transport, Macromolecules 33 (2000) 3185-3186.

[48] A. Morisato, Z. He, I. Pinnau, T.C. Merkel, Transport properties of PA12-PTMO/$AgBF_4$ solid polymer electrolyte membranes for olefin/paraffin separation, Desalination 145 (2002) 347-351.

[49] J.H. Kim, S.W. Kang, Y.S. Kang, Threshold silver concentration for facilitated olefin transport in polymer/silver salt membranes, J. Polym. Res. 19 (2012) 9753.

[50] R.D. Noble, C.A. Koval, Review of facilitated transport membranes, in: Y. Yampol'skii, I. Pinnau, B. Freeman (Eds), Materials science of membranes for gas and vapor separation, John Wiley & Sons, Hoboken, NJ, 2006, pp. 411-435.

[51] J.H. Kim, J. Won, Y.S. Kang, Olefin-induced dissolution of silver salts physically dispersed in inert polymers and their application to olefin/paraffin separation, J. Membr. Sci. 241 (2004) 403-407.

List of figure captions

Highlights:

Polymer/silver salt membranes for olefin/paraffin gas separation.

Fixed-site-carrier facilitated transport model to describe the olefin transport

Novel results of an experimental study at laboratory scale are reported.